2009 International Symposium on Intelligent Signal Processing and Communication Systems (ISPACS 2009) December 7-9, 2009

TP2-C-4

Noise-driven Image Processing based on Array-Enhanced Stochastic Resonance with Population Heterogeneity

Akira Utagawa* and Tetsuya Asai†

Graduate School of Information Science and Technology, Hokkaido University, Japan

* E-mail: utagawa@lalsie.ist.hokudai.ac.jp Tel: +81-11-706-7147

† E-mail: asai@ist.hokudai.ac.jp Tel: +81-11-706-6080

***Abstract*—We found a new class of stochastic resonance (SR) in a simple neural network that consists of i) photoreceptors generating nonuniform outputs for common inputs with random offsets, ii) an ensemble of noisy McCulloch-Pitts (MP) neurons each of which has random threshold values in the temporal domain, iii) local connections between the photoreceptors and the MP neurons with variable receptive fields (RFs), iv) the output cells, and v) local connections between the MP neurons and output cells. We calculated correlation values between the inputs and the outputs as a function of the RF size and intensities of the random components in photoreceptors and the MP neurons. We show the existence of "optimal noise intensities" of the MP neurons under the nonidentical photoreceptors and "nonzero optimal RF sizes", which indicated that optimal correlation values of this SR model were determined by two critical parameters; noise intensities (well-known) and RF sizes as a new parameter.**

I. Introduction

Stochastic resonance (SR) has recently been spotlighted in the field of engineering, which is motivated by a wide variety of sensing applications to detect weak signals [1]. Recent challenges in electrical engineering revealed that SR could be observed in a laser [2], [3], [4], nonlinear electrical circuits [5], [6], [7], sigma-delta modulators [8], quantum circuits [9], [10], [11], and so on. Noise and fluctuations are usually considered as "obstacles" in electrical systems. However, SR in electrical systems certainly exploited noises to improve the SNR, which implies that a new kind of electrical systems would be evolved by utilizing noise and fluctuations (*e.g.*, [12], [13], [14]).

Recently, Funke *et al.* reported that a visual pathway in a cat primary visual cortex optimally utilized an SR-like process to improve signal detection while preventing spurious noise-induced activity and keeping the SNR high [15]. Although the mechanism is still unclear, one may assume that i) SR without optimal tuning of noise intensities [16] underlies the fundamental mechanism and ii) the visual pathway from photoreceptors to cortical neurons may cause extremely large receptive fields (RFs). Inspired by these results and assumptions, we here propose a simple neural network model that consists of an array of SR units where threshold elements are represented by McCulloch-Pitts (MP) neurons and the MP neurons are shared by the neighboring SR units, *i.e.*,the number of MP neurons in each SR unit represents the RF size. Our primary interest here is to investigate the model's fundamental behaviors as a function of noise intensity, the RF size and population heterogeneity (random offsets between the inputs) that was not discussed in [15].

II. Neural Nets with Locally-Coupled SR Units

We here propose a simple neural network model for SR-based image processing. Our model accepts images (optical inputs), and generates the outputs through an SR process, as demonstrated in [9]. Three types of array structures of SR units are considered, as shown in Fig. 1. The first structure is illustrated in Fig. 1(a) where an optical input to a pixel is given to a single noisy MP neuron. Each neuron accepts temporal noises, and the temporal average of the neuron's output represents the pixel output. With this setup, the maximum correlation values between the input and the output would be low because the single pixel exactly corresponds to a SR network of $N = 1$ in [9]. To increase the correlation value, one can employ the second structure where multiple MP neurons are embedded in each pixel ($N = 3$ for example), as shown in Fig. 1(b). This setup certainly increases the correlation values, and the model would exhibit the best (but trivial) results with large N. Our interest here is to introduce receptive fields (RFs) in an array of SR units where MP neurons are shared by the neighboring SR units, as shown in Fig. 1(c). It should be noticed that an SR unit with $N = 3$ is hidden in this structure (illustrated by solid lines and circles in Fig. 1(c) left), and the MP neurons are shared by the neighboring SR units.

In Fig. 1(c), the optical input distribution is represented by $I(x)$, and is accepted by nominal photoreceptors. The output distribution of the photoreceptors is defined by $I(x) + \delta(x)$ where $\delta(x)$ represents the spatial random noise (pixel variations) given by $m \cdot N(0,1)$ [$N(0,1)$ is the Gaussian noise with zero mean and unity standard deviation]. Inputs to MP neurons via local coupling connections between photoreceptors and MP neurons were then defined by

$$R(x) = \int \big(I(X) + \delta(X)\big) \cdot g(X - x)\ dX, \qquad (1)$$

where σ and $g(x)$ represent the RF size and a normal distribution with variance σ^2 (zero mean), respectively. Output distribution of the MP neurons is thus

$$V(x) = H\big(R(x) - \xi(t)\big), \qquad (2)$$

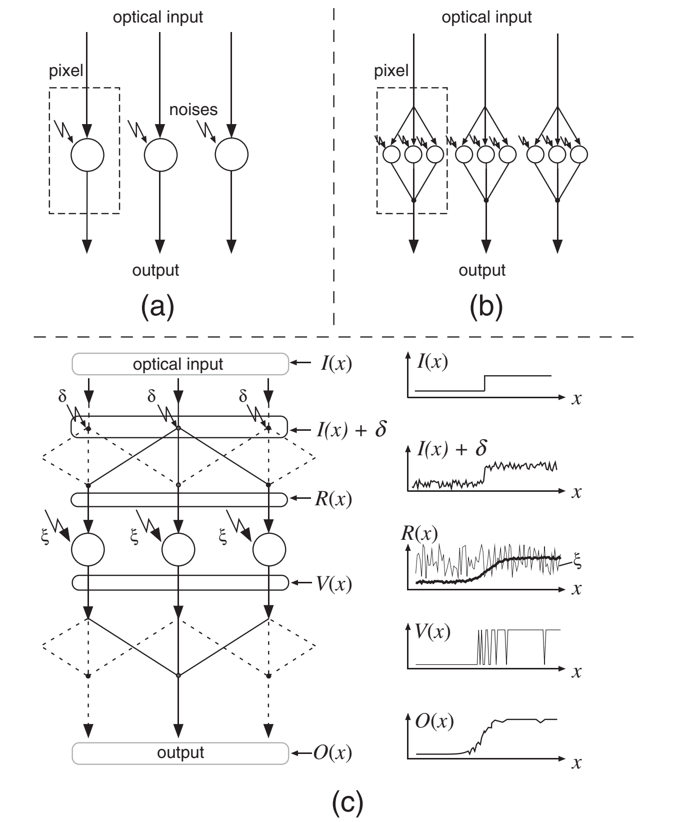

Fig. 1. Three types of SR models. (a) SR array with $N = 1$, (b) $N = 3$ and (c) proposed SR array having local connections where one pixel with $N = 3$ shown in (b) is hidden (solid lines and circles).

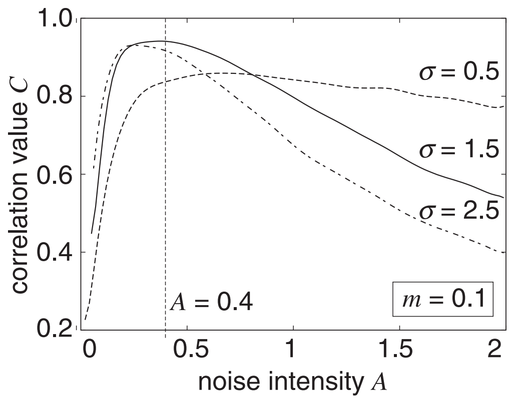

Fig. 2. Input-output correlations vs noise intensity.

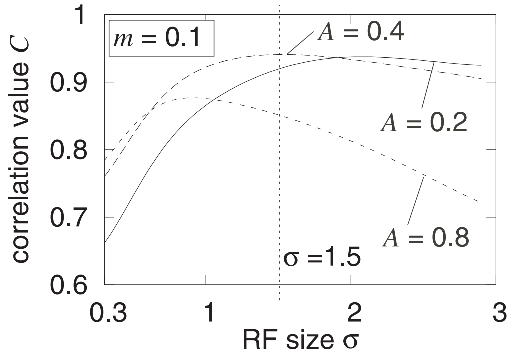

Fig. 3. Input-output correlations vs receptive-field size.

where $H(\cdot)$ represents a step function, and $\xi(t)$ the temporal random noise given by $A \cdot N(0, 1) + \theta$ (A: standard deviation, θ: mean threshold). The final output via local coupling connections between the MP neurons and the output cells is given by

$$O(x) = \int V(X) \cdot g(X - x)\, dX. \tag{3}$$

With this model, we examine SR behaviors by changing m (spatial randomness), σ (RF size), and A (temporal randomness being necessary for SR).

III. Results

We conducted numerical simulations to investigate effects of RF sizes and noises (random offsets in photoreceptors and temporal noises in MP neurons). In the following simulations, we assume $\theta = 0.5$ and $I(x) = 0.3 \cdot H(x - 0.5)$. The 1-D space ($x : [0, 1]$) is discretized with 32 MP neurons ($N = 32$) where $dx \equiv 1/N$ and $x = i \cdot dx$ (i: integer value). Figures 2 and 3 show plots of correlation values between the optical input $I(x)$ and final output $O(x)$ as a function of σ and A with different values of ms. The output $O(x)$ was obtained by averaging results of 512 trials with different random seeds. The correlation values were calculated by

$$C \equiv \frac{\sum_{i=1}^{N} [I(i \cdot dx) - \langle I \rangle] \cdot [O(i \cdot dx) - \langle O \rangle]}{\sqrt{\sum_{i=1}^{N} [I(i \cdot dx) - \langle I \rangle]^2} \sqrt{\sum_{i=1}^{N} [O(i \cdot dx) - \langle O \rangle]^2}}, \tag{4}$$

where $\langle I \rangle$ and $\langle O \rangle$ represent the spatially averaged distributions of $I(x)$ and $O(x)$ ($\langle I \rangle$ is 0.15, and $\langle O \rangle$ was numerically calculated from $O(x)$). The correlation values had a peak for variable noise intensity (A), as shown in Fig. 2. It should be noticed that the correlation values did not decrease suddenly as noise intensity A increased. When $\sigma = 1.5$, for example, the peak value was almost insensitive within $0.2 < A < 0.5$. Since σ qualitatively represents the number of neurons in the RF of each pixel, increasing σ may improve the correlation as in the basic SR network. However, nonzero σ causes smoothing of the optical input. Therefore there may exist upper bounds of σ. Figure 3 plots the correlation values as a function of σ. The peak value was obtained around $\sigma \approx 1.5$ and $A = 0.4$, which proves that nonzero σ (RF size) is necessary for obtaining higher correlation values in this SR system with nonidentical pixels ($m > 0$).

To confirm the effects of convergent coupling connections between $V(x)$ and $O(x)$ in our SR model, we calculated peak correlation values between $I(x)$ and $O(x)$ (C_{IO}) as well as correlation values between $I(x)$ and $V(x)$ (C_{IV}). Figure 4 plots the peak values as a function of spatial variance m ($I(x) = 0.1 \cdot H(x - 0.5)$). For given m, the peak values were

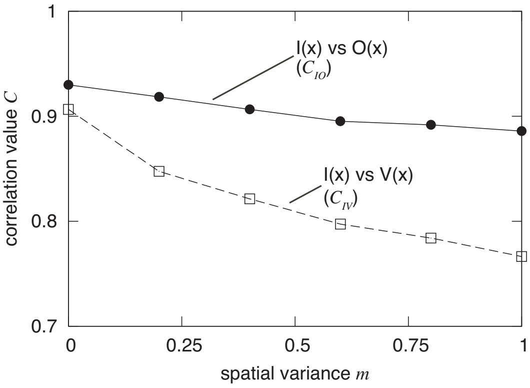

Fig. 4. Maximum correlation values vs spatial variance

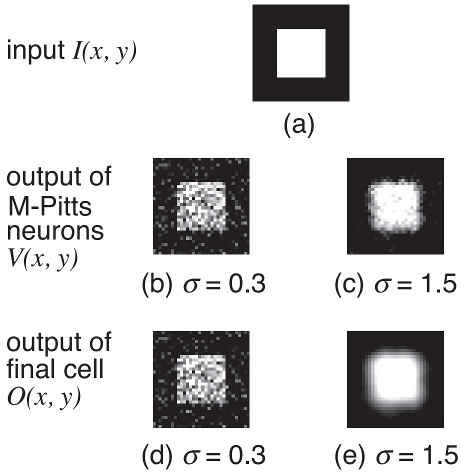

Fig. 5. 2-D simulation results with test pattern image. Gray-scale output images (b-e) were obtained by averaging binary results of 512 trials with different random seeds.

scanned by sweeping two parameters A (noise intensity) and σ (RF size). We observed an apparent difference between C_{IO} and C_{IV}, where C_{IO} was always larger than C_{IV}, and the difference expanded significantly as m increased. This result proves that employing the coupling connections between $V(x)$ and $O(x)$ is effective for increasing the correlation values, which results in improving quality of detected images.

Finally, we evaluated performances of a 2-D network with two distinct RF sizes ($\sigma = 0.3,\ 1.5$). Figure 5 shows the results ($A = 0.4$, $m = 0.1$, and $\theta = 0.5$). The binary input image $I(x, y)$ is shown in Fig. 5(a) [32×32-pixels black and white image. $I(x, y)$ = 0 (black) and 0.3 (white)], whereas level-adjusted density plots of outputs of neurons $V(x, y)$ [(b) and (c)] and final output cells $O(x, y)$ [(d) and (e)] with different RF sizes are shown. By comparing the final outputs of small RF ($\sigma = 0.3$) and relatively large RF ($\sigma = 1.5$), we first conclude that expanding RF sizes is useful for obtaining visually-better output image through SR among nonidentical pixels, if the input image is not complex (realistic). The important thing here is that the underlying mechanism of the performance increase mainly resulted from convergence on $O(x, y)$ with nonzero σ (=1.5), as proved in Fig. 4.

Figure 6 shows simulation results for realistic gray-scale input images. Figure 6(a) represents the input image [256×256-pixels 8-bit gray-scale image. $I(x, y)$s were re-normalized to 0 (black-most pixel) and 0.3 (white-most pixel)]. When $\sigma = 0.3$, the output image detected by SR was very noisy (Fig. 6(b)), which represents a raw image including random offsets detected by SR. Figures 6(c) and (d) show level-adjusted distributions of $V(x, y)$ and $O(x, y)$, respectively, when $\sigma = 1.5$. The difference in image qualities between Figs. 6(c) and (d) were not apparent at-a-glance view, however, there exists quantitative difference certainly, as shown in Fig. 4. It should be noted that when these image qualities are evaluated by using conventional indexes such as PSNR or correlation value, the difference among them is small.

IV. Discussion

We have shown that the maximum correlation value between input $I(x)$ and output $O(x)$ was obtained by setting optimal noise intensity A and receptive field (RF) size σ (Fig. 3). Figure 2 showed well-known SR characteristics, where subthreshold inputs $I(x)$ given to MP neurons were nominally amplified by applying temporal noises to the neurons. Moreover, a new type of SR was observed in Fig. 3 where maximum correlation value was obtained at certain value of RF size σ.

Here let us consider the reason why correlation value is maximized by non-zero σ. MP neurons receiving temporal noises may respond to subthreshold inputs if the sum of the inputs and the noise intensities exceed the threshold values. The response strongly depends on the noise sequences, *i.e.*, the neuron's output would be 1-bit temporal random sequences (time varying sequences of 0 and 1). When output $V(x)$ is averaged over time, the averaged value $\overline{V}$ converges to static values. If noises were applied to the neurons with optimal intensity, $\overline{V}$ converges to the subthreshold input, *i.e.*, $\overline{V}$ is strongly correlated with the input. Thus, the output of the MP neuron can be represented by its input.

Our model has two local-coupling layers, as shown in Fig. 1(c). One layer connects photoreceptors and MP neurons, and another connects the MP neurons and the output cell. Our results showed that these coupling connections (nonzero σ) were effective for decreasing spatial variance m in photoreceptors, which resulted in increase of correlation values between the noiseless input $I(x)$ and the model's output $O(x)$. The correlation value was non-monotonically increased as the RF size (σ) increased (Fig. 3). When m is increased, the correlation values would be decreased due to the nonzero σ. It should be noted that if $m = 0$, the maximum correlation value is certainly 1, however, the maximum value would be decreased as m increased because of the mismatches between $I(x) + \delta$ and output $O(x)$.

The network shown in Fig. 1(c) with small σ are considered to have the same characteristic as the conventional SR network shown in Fig. 1(a). Therefore, time-averaged output $\overline{O}$ in Fig. 1(c) is equal to the input of the MP neurons ($\overline{V}$),

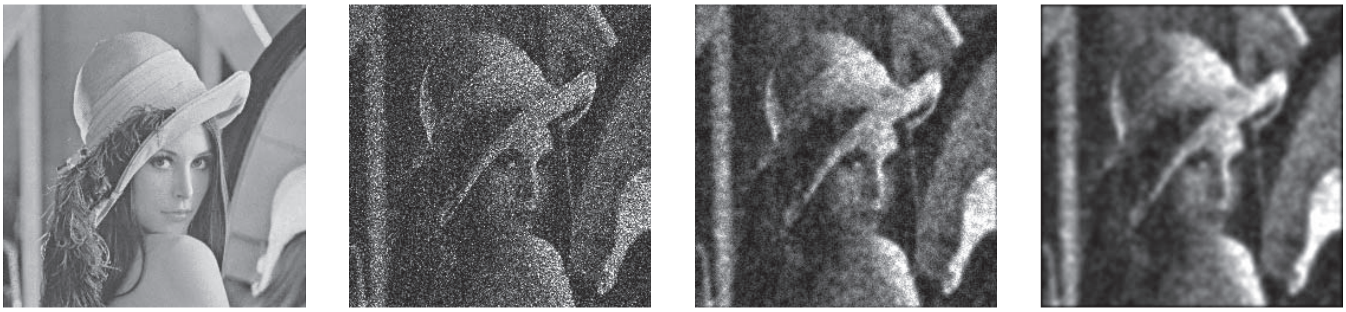

(a) input image $I(x, y)$ (256×256 8-bit gray-scale)

(b) output $O(x, y)$ with small RF ($\sigma = 0.3$)

(c) output $V(x, y)$ with large RF ($\sigma = 1.5$)

(d) output $O(x, y)$ with large RF ($\sigma = 1.5$)

Fig. 6. 2-D simulation results using gray-scale images. Grayscale output images (b-d) were obtained by averaging binary results of 512 trials with different random seeds.

as described above. Thus, when $m > 0$, $\overline{O}$ approaches to $I(x) + \delta(x)$. When m approaches to the signal level of $I(x)$, the correlation value between input $I(x)$ and output $O(x)$ ($\approx I(x) + \delta(x)$) would be low values. As σ increases, the correlation value is also increased because nonzero σ was effective for decreasing m, as described above. Further increase of σ results in the decrease of the correlation value. Remember that input distribution of MP neuron ($R(x)$) was defined by the convolution of $I(x) + \delta$ and coupling weight function $g(x)$ in Eq. (1). This means that, with extremely large σ, the spatial variance in $R(x)$ vanishes when a uniform $I(x)$ is given. On the other hand, the correlation value decreases due to the mismatches of $I(x)$ and extremely smoothed $O(x)$. Consequently, the spatial variance m is strongly suppressed by constructing the superimposed structure of SR units.

V. Summary

We proposed a simple neural network consisting of locally-coupled stochastic resonance (SR) units with nonidentical photoreceptors. Through numerical simulations, we observed a new class of SR among the units when the photoreceptors had random offsets. We calculated correlation values between the optical inputs and the output as a function of the receptive-field (RF) size and intensities of the random components in photoreceptors and the McCulloch-Pitts neurons. We then showed that there existed nonzero optimal sizes of the RF as well as optimal noise intensities of the neurons under the non-identical photoreceptors. Furthermore, we demonstrated 2D SR with the proposed model, and showed that the difference in image qualities between a simple-smoothing model with SR and smoothing-plus-convergent model with shared SR was not apparent at a glance, although there existed a quantitative difference between them.

Acknowledgment

This study was supported by a Grant-in-Aid for Scientific Research on Innovative Areas [20111004] from the Ministry of Education, Culture Sports, Science and Technology (MEXT) of Japan.

References

[1] F. Moss, L.L. Ward, and W.G. Sannita, “Stochastic resonance and sensory information processing: a tutorial and review of application,” *Clinical Neurophysiology*, vol. 115, pp. 267–281, 2004.

[2] V. Gautam and R. Rajarshi, “Stochastic resonance in a bistable ring laser,” *Phys. Rev. A*, Vol. 39, no. 9, pp. 4668–4674, 1989.

[3] A. Fioretti, L. Guidoni, R. Mannella, and E. Arimondo, “Evidence of stochastic resonance in a laser with saturable absorber: Experiment and theory,” *J. Statistical Phys.*, Vol. 70, No. 1–2, pp. 403–412, 2005.

[4] L. Zhang, “Stochastic resonance in a single-mode laser driven by quadratic pump noise and amplitude-modulated signal”, *Chinese Phys. B*, Vol. 18, pp. 1389–1393, 2009.

[5] F. Moss, J.K. Douglass, L. Wilkens, D. Pierson, and E. Pantazelou, Stochastic Resonance in an Electronic FitzHugh-Nagumo Model, Stochastic Processes in Astrophysics, J.R Buchler and H.E. Kandrup Eds., Annals of the New York Academy of Sciences, Vol. 706, The New York Academy of Sciences, New York, p. 26, 1993.

[6] V.S. Anishchenko, I.A. Khovanov, and B.V. Shulgin, “Stochastic resonance in passive and active electronic circuits”, *Chaotic, fractal, and nonlinear signal processing*, Vol. 375, pp. 363–381, 1996.

[7] O. Calvo and D.R. Chialvo, “Ghost stochastic resonance in an electronic circuit,” *Int. J. Bifurcation and Chaos*, Vol. 16, No. 3, pp. 731–735, 2006.

[8] O. Oliaei, “Stochastic resonance in sigma-delta modulators,” *Electronics Lett.*, Vol. 39, No. 2, pp. 173–174, 2003.

[9] T. Oya, T. Asai, and Y. Amemiya, “Stochastic resonance in an ensemble of single-electron neuromorphic devices and its application to competitive neural networks,” *Chaos, Solitons and Fractals*, Vol. 32, No. 2, pp. 855–861, 2007.

[10] S. Kasai and T. Asai, “Stochastic resonance in Schottky wrap gate-controlled GaAs nanowire field effect transistors and their networks,” *Applied Physics Express*, Vol. 1, 083001, 2008.

[11] S. Kasai, “Investigation on stochastic resonance in quantum dot and its summing network,” *Int. J. Nanotechnology and Molecular Computation*, Vol. 1, No. 2, pp. 70–79, 2009.

[12] T. Oya, I.N. Motoike, and T. Asai, “Single-electron circuits performing dendritic pattern formation with nature-inspired cellular automata,” *Int. J. Bifurcation and Chaos*, Vol. 17, No. 10, pp. 3651–3655, 2007.

[13] A. Utagawa, T. Asai, T. Hirose, and Y. Amemiya, “An inhibitory neural-network circuit exhibiting noise shaping with subthreshold MOS neuron circuits,” *IEICE Trans. Fundamentals*, Vol. E90-A, No. 10, pp. 2108–2115, 2007.

[14] A. Utagawa, T. Asai, T. Hirose, and Y. Amemiya, “Noise-induced synchronization among sub-RF CMOS analog oscillators for skew-free clock distribution,” *IEICE Trans. Fundamentals*, Vol. E91-A, No. 9, pp. 2475–2481, 2008.

[15] K. Funke, N.J. Kerscher, and F. Wörgötter, “Noise-improved signal detection in cat primary visual cortex via a well-balanced stochastic resonance like procedure,” *European J. Neuroscience*, Vol. 26, No. 5, pp. 1322–1332, 2007.

[16] J.J. Collins, C.C. Chow, T.T. Imhoff, “Stochastic resonance without tuning,” *Nature*, Vol. 376, pp. 236–238, 1995.